Virology 379 (2008) 10–19

Contents lists available at ScienceDirect

Virology

journal homepage: www.elsevier.com/locate/yviro

Biochemical and structural characterisation of membrane-containing icosahedral dsDNA bacteriophages infecting thermophilic *Thermus thermophilus*

S.T. Jaatinen, L.J. Happonen, P. Laurinmäki, S.J. Butcher, D.H. Bamford *

Department of Biological and Environmental Sciences and Institute of Biotechnology, Biocenter 2, FIN-00014, University of Helsinki, Finland

ARTICLE INFO

Article history:
Received 1 February 2008
Returned to author for revision11 March 2008
Accepted 8 June 2008
Available online 25 July 2008

Keywords:
P23-77
P23-72
P23-65H
Thermus
Thermus thermophilus
Bacteriophage
Thermophilic
Membrane-containing

ABSTRACT

Icosahedral dsDNA viruses isolated from hot springs and proposed to belong to the *Tectiviridae* family infect the Gram-negative thermophilic *Thermus thermophilus* bacterium. Seven such viruses were obtained from the Promega Corporation collection. The structural protein patterns of three of these viruses, growing to a high titer, appeared very similar but not identical. The most stable virus, P23-77, was chosen for more detailed studies. Analysis of highly purified P23-77 by thin layer chromatography for neutral lipids showed lipid association with the virion. Cryo-EM based three-dimensional image reconstruction of P23-77 to 1.4 nm resolution revealed an icosahedrally-ordered protein coat, with spikes on the vertices, and an internal membrane. The capsid architecture of P23-77 is most similar to that of the archaeal virus SH1. These findings further complicate the grouping of icosahedrally-symmetric viruses containing an inner membrane. We propose a single superfamily or order with members in several viral families.

Introduction

Comparisons of high resolution capsid structures of viruses have led to a surprising observation that viruses considered to be unrelated and even infecting hosts in different domains of life (bacteria, archaea, eukarya) show strong structural conservation in their virion architecture (Bamford et al., 2005a; Benson et al., 2004). Tectiviruses (type organism enterophage PRD1) are dsDNA phages with an internal membrane vesicle that encloses the dsDNA genome (Bamford, 2005). There are Tectiviruses infecting both Gram-negative and Gram-positive bacterial hosts (Ravantti et al., 2003). Based on related coat protein fold and virion architecture several viruses infecting archaeal and eukaryotic hosts share these properties with the Tectiviruses. It has been postulated that such viruses have a common origin forming a lineage or clade composed of structurally related viruses with a double β-barrel coat protein fold (Bamford et al., 2005a; Benson et al., 2004). The viruses apart from Tectiviruses belonging to this lineage are adenovirus, although it does not have an internal membrane (Benson et al., 1999), Paramecium bursaria chlorella virus 1 (PBCV-1; (Nandhagopal et al., 2002), and *Sulfolobus* turreted icosahedral virus (STIV; (Khayat et al., 2005). A hypothesis has been put forward that viruses may be ancient, already infecting early cells prior to the separation of the current domains of cellular life (Bamford et al., 2002).

Very recently we have determined the structure of the halophilic, icosahedral, membrane-containing archaeal dsDNA virus SH1 using cryo-EM and three-dimensional image reconstruction (Jäälinoja et al., 2008). It has an unusual triangulation number (T=28) but in contrast to the PRD1-like viruses, it appears that SH1 has hexagonal capsomers, that appear to be formed of six individual β-barrels instead of three double β-barrels. The capsomers of SH1 are decorated by additional proteins in a conformation-dependent fashion.

Thermus bacteria, with optimal growth temperatures of 70–75 °C, are found in alkaline hot springs, hot water heaters and natural waters subjected to thermal pollution (Hreggvidsson et al., 2006; Pask-Hughes and Williams, 1975; Ramaley and Hixson, 1970). *Thermus* cells have an outer membrane and a peptidoglycan layer in their cell envelope and are thus structurally similar to Gram-negative bacteria, although they reside in the *Thermus–Deinococcus* phylum (Brock, 2005). Thermophilic bacteria and their phages have been actively studied due to their potential for biotechnological applications. Such studies have focused on the exploitation of their enzymes, RNA, ribosomes and protein synthesizing machineries (Pantazaki et al., 2002).

About 5600 bacteriophages have been described so far (Ackermann, 2007), but only a few reports have been published on those infecting *Thermus* species. The first reported isolate was the tailed icosahedral dsDNA phage phi-YS40 infecting *T. thermophilus* HB8 (Sakaki and Oshima, 1975). Other isolates have also been reported, e.g.

* Corresponding author. Viikki, Biocenter, P.O. Box 56 (Viikinkaari 5), FIN-00014, University of Helsinki, Finland. Fax: +358 9 19159098.
E-mail address: dennis.bamford@helsinki.fi (D.H. Bamford).

0042-6822/$ – see front matter © 2008 Elsevier Inc. All rights reserved.
doi:10.1016/j.virol.2008.06.023

the filamentous phage PH75 infecting *T. thermophilus* (Pederson et al., 2001) as well as phage TS2126 infecting *T. scotoductus* (Blondal et al., 2005). The most extensive survey so far conducted was done by the Promega Corporation in which 115 bacteriophages, apparently belonging to the *Myoviridae*, *Siphoviridae*, *Tectiviridae*, and *Inoviridae* families, were obtained from alkaline hot springs in New Zealand, Russia and the U.S.A. (Yu et al., 2006). We examined seven icosahedral, nontailed, dsDNA phages infecting *Thermus* species, originating from the Promega collection. Three of them, were closely related and grew to high titer. One of them, P23-77, was studied further and had lipids as virion components. It was shown by electron cryo-microscopy (cryo-EM) and three-dimensional image reconstruction to be closely related to other icosahedrally-symmetric dsDNA viruses with an internal membrane resembling most closely the archaeal virus SH1 (Jäälinoja et al., 2008).

Results

Comparison of phages P23-77, P23-72 and P23-65H

We initially obtained seven tailless icosahedral dsDNA virus specimens from the Promega collection. We were able to grow three of them (P23-77, P23-72, P23-65H) to high titers ($>1\times10^{11}$ pfu/ml agar stocks) and these were analysed further. These viruses originate from the North Island of New Zealand (Yu, Slater, and Ackermann, 2006). Plaques were fully developed after 16 h at 70 °C; the diameter of the clear plaques was 0.5–2 mm depending on the humidity during incubation. The infection was most efficient when the host cells were in the logarithmic growth phase ($\sim7\times10^{8}$ cfu/ml). The cells were susceptible to the phages for up to 4 h if stored at room temperature where no further growth occurred.

In the single cycle growth experiment, the culture turbidity started to decrease ~90 min p.i. yielding $\sim1\times10^{11}$ pfu/ml in the supernatant and giving an average burst size of ~200 pfu/cell (Fig. 1A). All three phages had practically identical growth cycles and yields. They also appeared indistinguishable in negative stain (not shown) and thin-section electron microscopy as shown in Fig. 1B. Virus particles were seen associated with the cell surface at 15 min p.i. similarly for all three viruses. After 45 min p.i. progeny viruses were visible in cell interiors, and 70 min p.i. lysing cells were detected. The maximal adsorption (~70%) was reached in about 10 min at 70 °C (shown for P23-77 in Fig. 1C) giving an adsorption rate constant of 1.7×10^{-10} ml/min (using 5 min p.i. time) (Adams, 1959). At room temperature, the maximal adsorption was about 60% and the adsorption rate constant was 7.3×10^{-11} ml/min when determined 10 min p.i.

Phages P23-77, P23-72 and P23-65H were concentrated and purified by rate zonal (1× purified) and equilibrium (2× purified) centrifugations and the pelleted 2× purified particles were subjected to SDS-PAGE analysis (Fig. 2). The protein profiles were very similar but not identical between the viruses. The virions have two major protein species with apparent molecular masses of about 20 and 35 kDa respectively.

To determine the optimal storage temperature the virus stocks were stored at 37 °C, 28 °C, 22 °C, 4 °C and their infectivities were assayed. P23-77 and P23-72 were most stable at 28 °C and P23-65H at 22 °C (not shown). The stability of the three viruses was further determined by assaying the virus stock infectivity periodically at the determined optimal storage conditions. P23-72 and P23-65H both suffered from a drop in titre over a 72 h period, whereas P23-77 was not affected. However, when P23-77 was incubated at 70 °C ~70% of its infectivity was lost in 24 h. Due to its superior stability P23-77 was chosen for further analyses.

Properties of phage P23-77

P23-77 virus has a tendency to aggregate upon concentration and purification. We established optimal buffer components using a multivariate search of conditions for maximal solubility and stability based on the titer after resuspension of PEG-concentrated viruses in different buffer conditions. Our optimal buffer contains 20 mM Tris–HCl, pH 7.5, 5 mM $MgCl_2$ and 150 mM NaCl. To avoid aggregation PEG-concentrated virus was resuspended in no less than 1/20 of the original lysate volume.

Rate zonal ultracentrifugation (linear 5–20% sucrose gradient) gave only a single virus-containing band composed mainly of DNA-containing virions. Based on cryo-EM we estimated that only 2% of the particles were empty. When the virus zone from the rate zonal centrifugation was analyzed by equilibrium centrifugation a sharp infectious virus zone was obtained at a density of 1.22 g/ml sucrose (Fig. 3A) and 1.21 g/ml CsCl (not shown). The recovery of infectious viruses during the purification process is shown in Table 1. The specific infectivity based on protein concentrations determined by the Bradford assay (Bradford, 1976) was $\sim4\times10^{12}$ pfu/mg protein for the 1× virus and $\sim3\times10^{12}$ pfu/mg protein for the 2× virus (in sucrose). In both cases the collection of viruses from gradient fractions by differential centrifugation led to about a 50% decrease in specific infectivity.

Due to the low buoyant density, we expected P23-77 to contain lipids. Consequently we determined the distribution of neutral lipids in the equilibrium centrifugation fractions by thin layer chromatography (Fig. 3B). The majority of lipids found in *T. aquaticus* are neutral lipids (Ray et al., 1971). Neutral lipids were detected only in fractions containing the highly purified infectious virus particles. We analysed the major viral proteins in the purified virus preparation by tricine-SDS-PAGE (Fig. 3C) (Schägger and von Jagow, 1987) that better separated the P23-77 virion proteins than our standard SDS-PAGE (Fig. 2). There are 10 identifiable protein species with apparent masses ranging from 8 to 35 kDa of which two are major bands (apparent molecular masses 20 and 35 kDa). The proteins larger than 35 kDa did not peak with the virus in the sucrose gradients, and are thus probably host-derived (Fig. 3). Also the comparison to highly purified SH1 virion protein pattern is depicted in Fig. 3C. SH1 has two major coat proteins VP4 (25.7 kDa) and VP7 (20.0 kDa) (Bamford et al., 2005b) although they migrate anomalously in gel electrophoresis (Fig. 3C).

Electron cryo-microscopy and image reconstruction of P23-77

We analysed purified P23-77 virions from 1× and 2× purified sucrose zones using cryo-EM and three-dimensional image reconstruction in order to further characterize the virion. The majority of the P23-77 viral particles seen in the electron micrographs were spherical, intact, DNA-filled virions (Fig. 4A, white arrow). Very rarely, a few similar-sized DNA-lacking (empty) particles were also observed (Fig. 4A, inset). Approximately 15 nm long stick-like spikes can be seen extending from the surface of some of the virions (Fig. 4A, black arrows).

An icosahedral three-dimensional reconstruction of intact particles to 1.4 nm resolution was calculated from 880 images using 25 micrographs (underfocus range 1.0–3.0 μm; Figs. 4B and 5A). In addition, a reconstruction of empty particles to 3.0 nm resolution was calculated from 49 images taken from 44 CCD-micrographs (not shown). The two types of particles were highly spherical, and of the same size with an average diameter of 78 nm (Fig. 4C).

The three-dimensional reconstruction of intact P23-77 particles revealed an icosahedrally-symmetric multilayered structure consisting of an outer protein capsid (6 nm thick) with several underlying layers (Fig. 4B). To determine which layers belong to DNA, we compared radial profiles calculated from the intact and empty particle reconstructions (Fig. 4C). Since the two types of particles were of the same size, we could identify that the membrane which follows the shape of the capsid, resides directly underneath the capsid (radii 25.5–

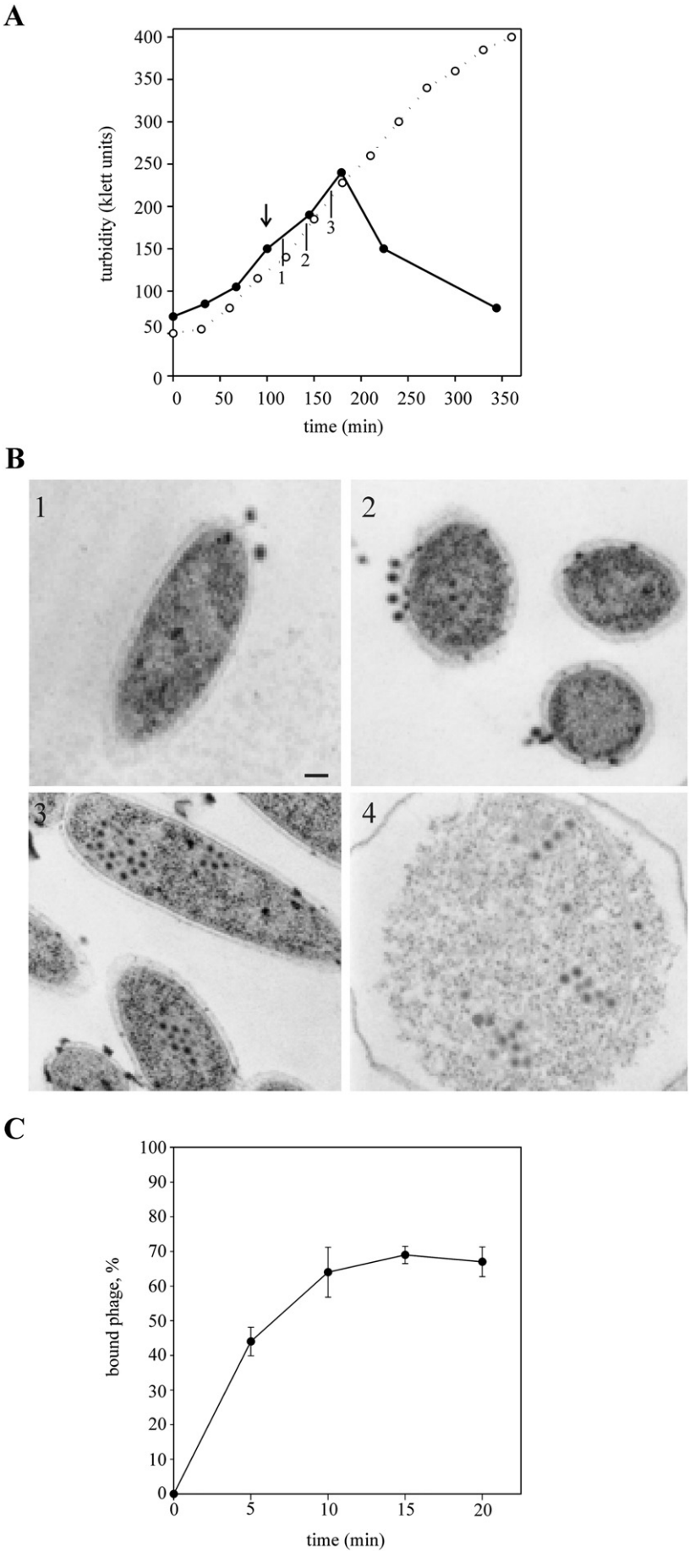
A
turbidity (klett units)
time (min)
1
2
3
B
1
2
3
4
C
bound phage, %
time (min)

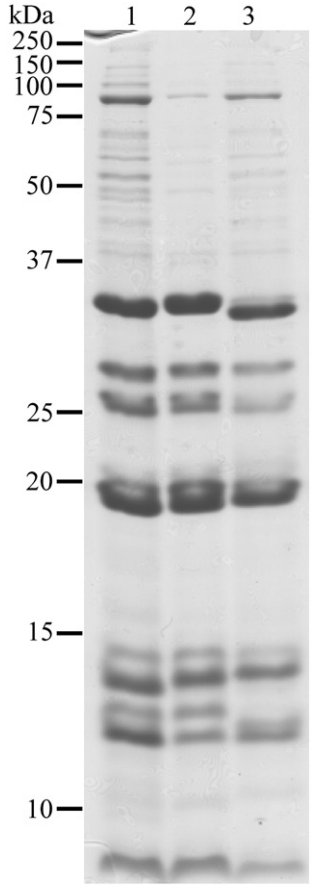

Fig. 2. Protein profiles of purified thermus phages P23-65H (lane 1), P23-72 (lane 2) and P23-77 (lane 3). Protein mass markers are indicated on the left.

28.5 nm in Fig. 4C) and the remaining layers towards the center of the virion are DNA (radii 4–22 nm in Fig. 4C). The DNA forms concentric rings separated by an average of 3.1 nm (peak to peak distance; Fig. 4C).

Capsid and capsomer arrangement of P23-77

The triangulation (T) number defines the number of pseudo-identical subunits with quasi-similar environments in an icosahedral asymmetric unit (Caspar and Klug, 1962). In P23-77 the capsid lattice is $T=28$ (Fig. 5A). The capsid of P23-77 consists of 270 hexameric (4.5 per asymmetric unit) and 12 pentameric capsomers (Figs. 5A, C and E and 6; pentamers in yellow) as in SH1 (Figs. 5B, D, F) — the only other virus, for which such a T-number has been described (Jäälinoja et al., 2008).

The surface of the capsid is covered in small protruding towers. Two towers are attached to each hexameric capsomer base (Figs. 5C, E and 6). The position of the towers depends on the position of the capsomer in the shell lattice (Fig. 6). The towers are located either on the same side of the hexameric base (green and red capsomers in Figs. 5A and 6; type A capsomers) or on opposite corners (blue capsomers in Figs. 5A and 6; type B capsomers). The average mass of both type A and B capsomers calculated from segmented volumes is 150 kDa. The red type A capsomers are rotated 60° relative to the green type A capsomers in the same asymmetric unit (Fig. 6E). SH1 also has such protruding towers, but the number and position differ to those of P23-77 (Figs. 5A, B and E, F). In SH1 the number of towers can be three (compare red and green spots in Figs. 5E, F) or two (compare blue spots in Figs. 5E, F). If we compare the P23-77 and SH1 capsomers closer to the base (radii of 37 and 38 nm, Figs. 5C, D), the P23-77 capsomers appear rounder and more regular than those of SH1. In SH1 the two capsomer types are clearly distinct, either with a more triangular base (red and green in Figs. 5B–D) or a skewed base (blue in Figs. 5B–D). In SH1 the decorating towers are clearly arranged in a conformation-dependent manner depending on the base (Jäälinoja et al., 2008). In contrast, in P23-77 the number of towers depends on the position of the capsomer in the asymmetric unit, however the net effect is the same, that there are two classes of capsomers, arranged similarly in the two viruses. In both SH1 and P23-77 the individual capsomers appear to be hollow, as is commonly seen for β-barrel structures at this resolution.

Pentameric bases, most probably composed of a separate protein, have an estimated mass of 90 kDa with spikes attached, occupy the vertices (Fig. 5; marked in yellow). The spikes seen in the micrographs (Fig. 4A, black arrows) appear shorter in the icosahedral reconstruction (Fig. 4B and Fig. 7A), which could be due to low occupancy, flexibility, and/or inappropriate averaging in the icosahedral reconstruction process (Fig. 7A; (Briggs et al., 2005; Huiskonen et al., 2007a, 2007b). The spikes protruding from the capsid surface are straight, thin and narrow in P23-77 (Fig. 7A), but bifurcated, two-fold symmetric and very large in SH1 (Fig. 7B; Jäälinoja et al., 2008). In both viruses, proteins anchor the capsid to the membrane at the five-fold vertices. In SH1, these are transmembrane proteins (Jäälinoja et al., 2008), but appear to be peripheral membrane proteins in P23-77 (Fig. 7).

Discussion

The dominant viruses in aquatic environments are icosahedral tailed dsDNA phages. Interestingly, when high temperature aquatic environments are studied the dominant isolates are tailless icosahedral and filamentous viruses infecting both bacterial and archaeal hosts (Rachel et al., 2002; Romancer et al., 2007). Here we investigated icosahedral tailless DNA phages from hot springs in New Zealand that were the dominant class of viruses infecting thermophilic *Thermus* bacteria residing in the *Thermus–Deinococcus* phylum (Yu et al., 2006).

We compared three independent isolates of tailless icosahedral *Thermus* viruses. All three efficiently infected the host. To our surprise, highly purified virions produced similar protein patterns with small changes in the mobility of several protein bands (Fig. 2). However, there were considerable differences in the virion stability between the studied viruses. It appears that the hot spring environment favors micro variability in the tailless Thermus phage community. For the most stable of these viruses (P23-77) optimized prod
uction and purification methods were developed (Table 1). The specific infectivity of $\sim 4\times10^{12}$ pfu/mg protein obtained is close to the values obtained for membrane-containing phages PRD1 and PM2 (Bamford and Bamford, 1991; Kivela et al., 1999) indicating that we have succeeded in producing highly infectious P23-77. We also observed here that although the optimal temperature for the host and phage adsorption is ~70 °C, the viruses studied here were most stable at moderate temperatures between 22 and 28 °C and also adsorbed readily to the host cell at such temperatures. It appears that these phages have adapted to strong temperature fluctuations in their environments.

Fig. 1. (A) Single cycle growth curve of P23-77 phage. The growth of uninfected cells is marked with open circles and the infected ones with closed circles. The infection time is indicated with an arrow. The sampling times for thin-section electron microscopy are indicated by 1, 2 and 3. (B) Electron micrographs of thin sectioned *T. thermophilus* cells infected with phage P23-77, P23-72 or P23-65 H. Cells harvested 15 (1, P23-77) and 45 min (2, P23-72) and 70 min (3, P23-77; 4, P23-65H) p.i.. Scale bar represents 100 nm. (C) Binding of P23-77 to *T. thermophilus* cells at 70 °C.

We show that these *Thermus* viruses contain lipids organized as a bilayer underneath the protein capsid. The large lipid-containing viruses, like PBCV-1 and Chilo iridescent virus (Huiskonen and Butcher, 2007), have their double β-barrel, pseudo-hexameric capsomers arranged as trigonal arrays forming the facets of the virus (Abrescia et al., 2004; Nandhagopal et al., 2002; Simpson et al., 2003; Yan et al., 2000). It was observed by Wrigley that when such viruses were dissociated, triangular "trisymmetrons" and pentagonal "pentasymmetrons" were visible (Wrigley, 1969). Detailed analysis of the capsomer packing in PBCV-1 and Chilo iridescent virus from fitting of the capsomer X-ray structure into EM reconstructions, shows that a capsomer in the pentasymmetron is rotated by 72° relative to its neighbouring pentasymmetron capsomer, and 60° relative to the adjacent trisymmetron capsomer; two interaction types with very different buried surface areas (Simpson et al., 2003). The pseudo-hexameric capsomers in trisymmetrons are similarly oriented to each other with one interaction type (Simpson et al., 2003). It has been observed that for *T*-numbers where *h* is odd, adjacent trisymmetrons make contact across the two-fold axis of symmetry. However, when *h* is even Wrigley predicted that linear disymmetrons would be required to form the contacts between trisymmetrons (Simpson et al., 2003; Wrigley, 1969). In the case where both *h* and *k* are even e.g. *T*=28, the central capsomer of the disymmetron would sit on the icosahedral 2-fold axis of symmetry. In such a case a virus with trimeric capsomers would either have to abandon icosahedral symmetry or use a special two- or six-fold symmetric capsomer (Simpson et al., 2003). In P23-77 and SH1 we see the first examples, to our knowledge, of viruses containing linear disymmetrons, formed from the B type capsomers (Figs. 5A and B, blue capsomers). As predicted, the central capsomer is two-fold symmetric, but interestingly, so are the other disymmetron capsomers on either side. The pentasymmetrons (red in Figs. 5A, 5B and 6E), now have an additional interaction with the adjacent disymmetron capsomer (Fig. 6E). The P23-77 capsomers belonging to the trisymmetron (green in Figs. 5A and 6E) are not pseudo-hexameric, and only face in the same direction within the asymmetric unit, rotating 120° around the icosahedral three-fold axis of symmetry. This is not apparent in SH1 or PBCV1-1 where the trisymmetron capsomers are pseudo-hexameric. The Wrigley scheme was originally introduced in the context of the assembly of very large viruses, and there the natural interpretation for the occurrence of di-, tri- and pentasymmetrons was as intermediates in virus assembly. In the case of a relatively small capsid this may not be true, but it does remind us of the differences in buried surface area that may occur between capsomers in different areas of the asymmetric unit assigned to di-, tri- or pentasymmetrons. These different interactions are potential sites for

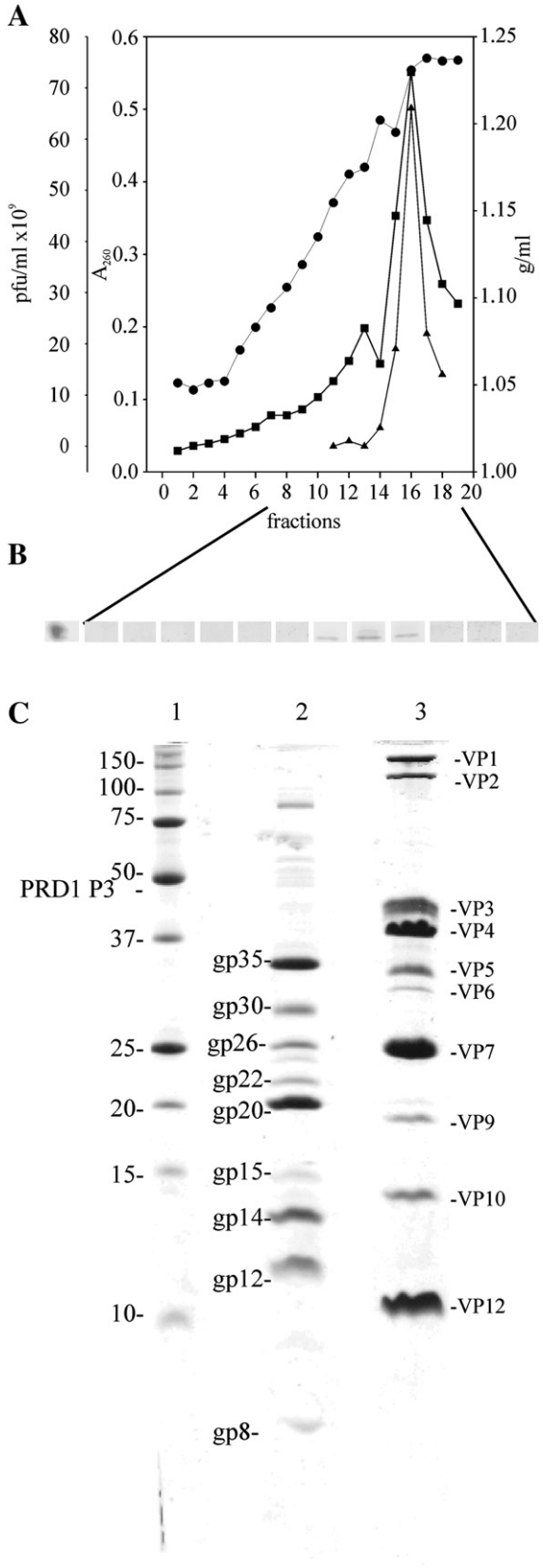

Fig. 3. (A) Purification profile of P23-77 in a 20–70% equilibrium sucrose gradient. The density of the gradient fractions (g/ml, circles), A_{260}, (squares) and infectivity (pfu/ml, triangles) are depicted. (B) Thin-layer chromatograms of neutral lipids of fractions 8–19, the first lane is 2× purified P23-77. (C) Tricine SDS-PAGE gel comparing a protein marker (lane 1) with the protein profile from the P23-77 pooled peak infectivity fractions (14–17; lane 2) and highly purified SH1. P23-77 proteins are designated according to their apparent molecular masses. SH1 proteins are indicated, the major SH1 capsomer proteins are VP4 (25.7 kDa) and VP7 (20.0 kDa). The position where the PRD1 major coat protein P3 (43.1 kDa) migrates is indicated to the left of lane 1.

Table 1
Recovery of bacteriophage P23-77 during concentration and purification steps in sucrose

	Recovery of infectivity (pfu/Litre of starting culture)	Recovery of infectivity (%)	Specific infectivity (pfu/mg protein)
Cell lysate	1.2×10^{14}	100	–
PEG precipitate	8.3×10^{13}	69	–
1× virus gradient band	4.5×10^{13}	38	8.2×10^{12}
1× virus pelleted	2.3×10^{13}	19	4.2×10^{12}
2×virus gradient band	2.0×10^{13}	17	5.6×10^{12}
2× virus pelleted	9.2×10^{12}	8	3.1×10^{12}

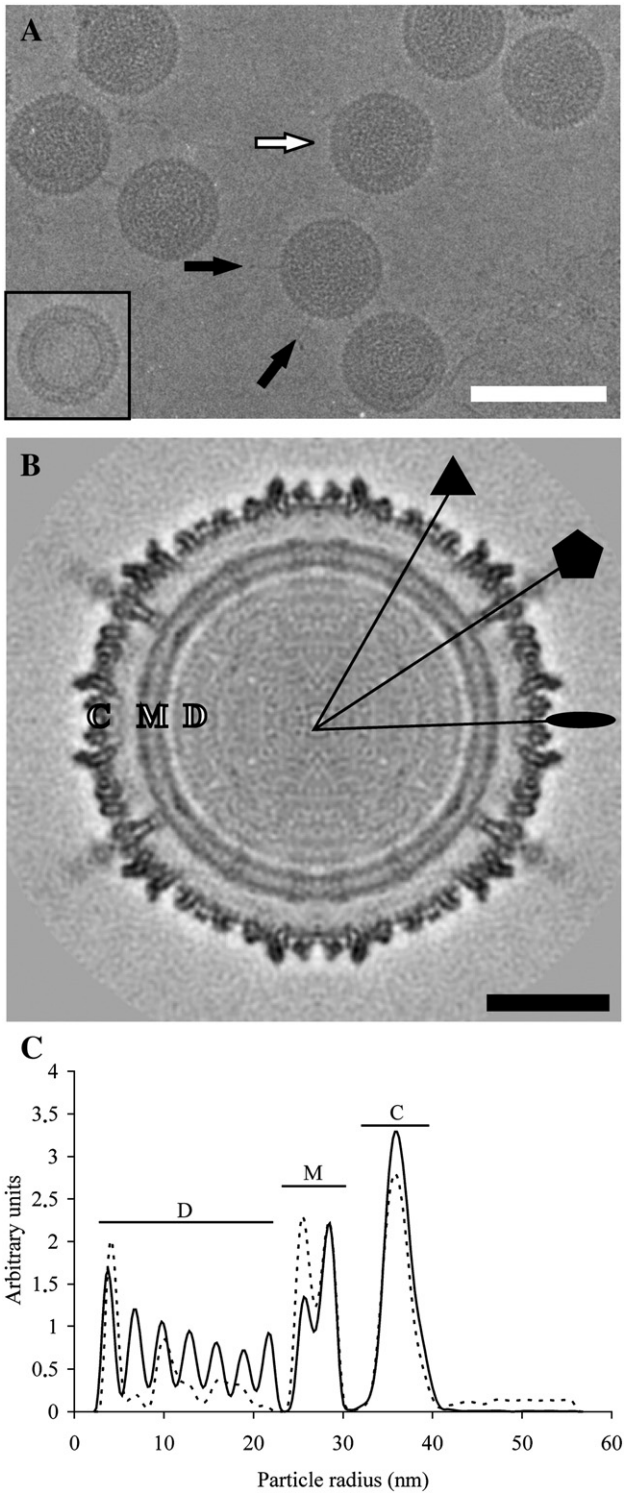

Fig. 4. (A) Organization of P23-77. Cryo-electron micrograph taken at 2.7 μm underfocus showing P23-77 viral particles (white arrow), with a diameter of 78 nm. Thin spikes, which might be used in the infection of the host, are visible on some particles (black arrow). The viral membrane inside the protein capsid is visible in empty particles (inset, underfocus 2.2 μm). Bar, 100 nm. (B) A 0.28 nm thick central section through the virion. Symmetry axes are indicated with a black ellipse (2-fold), triangle (3-fold) and pentagon (5-fold). Proteins connecting the viral capsid and the underlying lipid bilayer at the five-fold vertexes are visible. D (DNA), M (membrane) and C (capsid shell). Bar, 20 nm. Protein is black in A and B. (C) Radial density profiles of the icosahedral reconstruction of the intact virion (solid line) and the empty particle (dotted line). For calculation of the radial profiles both the full and the empty particle reconstructions were calculated to 3.0 nm resolution.

interactions with minor capsid proteins important in regulating assembly, e.g. in PRD1 there is an elongated, dimeric, minor protein running between adjacent facets at the junction between two trisymmetrons (Abrescia et al., 2004). In P23-77 it seems likely that the capsomers are built from two different protein species, one forming the hexagonal bases, and the other the towers. The tower protein binding is related to the position of the underlying capsomer in the asymmetric unit. Two major bands (gp 20 and 35) are seen in SDS-PAGE analysis of P23-77 particles. They are of an appropriate molecular weight and abundancy to be constituents of the capsomers. Whether we are dealing with trimeric or hexameric capsomers is intriguing. Obviously higher resolution data is needed to unequally determine this. Given the occurrence of the type B capsomers (Figs. 5 and 6), it is most likely that the capsomer has 6 subunits in the base, as was concluded for SH1 (Jäälinoja et al., 2008).

P23-77 has pentamers at the five-fold vertices, to which the spikes are attached. The average mass for the pentamer is 90 kDa, which gives a mass of 18 kDa for the monomeric protein. This value resembles those for the viruses of the PRD1-type such as Bam35, SH1, PRD1 and STIV (Abrescia et al., 2004; Jäälinoja et al., 2008; Laurinmaki et al., 2005; Rice et al., 2004). Based on SDS-PAGE analysis (Fig. 3C), there are three protein bands with apparent molecular weights between 15–22 kDa, that could form the pentamer. P23-77 has long narrow spikes on the vertices reminiscent of the receptor binding complex in PRD1 (Huiskonen et al., 2007b). It is likely that the P23-77 spikes are involved in host attachment. The P23-77 spikes are quite dissimilar to the horn-like spikes of SH1 (Jäälinoja et al., 2008) or the turreted spikes of STIV (Maaty et al., 2006) which both have archaeal hosts. Hence spike protein evolution tends to reflect host specificity rather than reflecting the evolution of the capsid proteins.

Tectiviruses have membrane-containing procapsids that are packaged by a viral ATPase without capsid expansion (Grahn et al., 2006). In P23-77, very few empty particles were identified in the purified virus preparation and no empty particle band was observed during gradient purification of cell lysates. This could indicate that packaging is very rapid and efficient in P23-77, that procapsids are very unstable under our purification conditions, or that the virus does not go through a procapsid intermediate. The DNA in the capsid of P23-77 is highly ordered and the spacing between the concentric DNA rings is 3.1 nm. This spacing is relatively low compared to that of the other dsDNA bacteriophages T7, P22 and PRD1, where the average spacing of the concentric DNA layers is approximately 2.5 nm (Cerritelli et al., 1997; Chang et al., 2006; Cockburn et al., 2004). The P23-77 membrane localization and organization are similar to that which has been observed in other membrane-containing bacteriophages PRD1, Bam35 (*Tectiviridae*) and PM2 (*Corticoviridae*) and the archaeal viruses STIV and SH1 (Abrescia et al., 2004; Huiskonen et al., 2004; Jäälinoja et al., 2008; Laurinmaki et al., 2005; Rice et al., 2004).

The discovery of two viruses, one infecting an archaeal and the other a bacterial host with similar capsid architecture reminiscent to, but deviating from, the canonical PRD1 architecture, is surprising and intriguing. Whether these *Thermus* phages can be positioned in the *Tectiviridae* family remains an open question. As the closest structural relative to P23-77 is an archaeal virus and as the PRD1 virion has its closest structural counterparts in viruses infecting archaeal and eukaryotic hosts, we hope that further structural analyses reaching to higher resolution will shed more light on the relatedness of these viruses with an internal membrane.

Materials and methods

Bacteria and phages

The icosahedral nontailed phages (P23-65H, P23-72, P23-77, P37-14, P78-65, P78-83 and P78-86) were obtained from the Promega

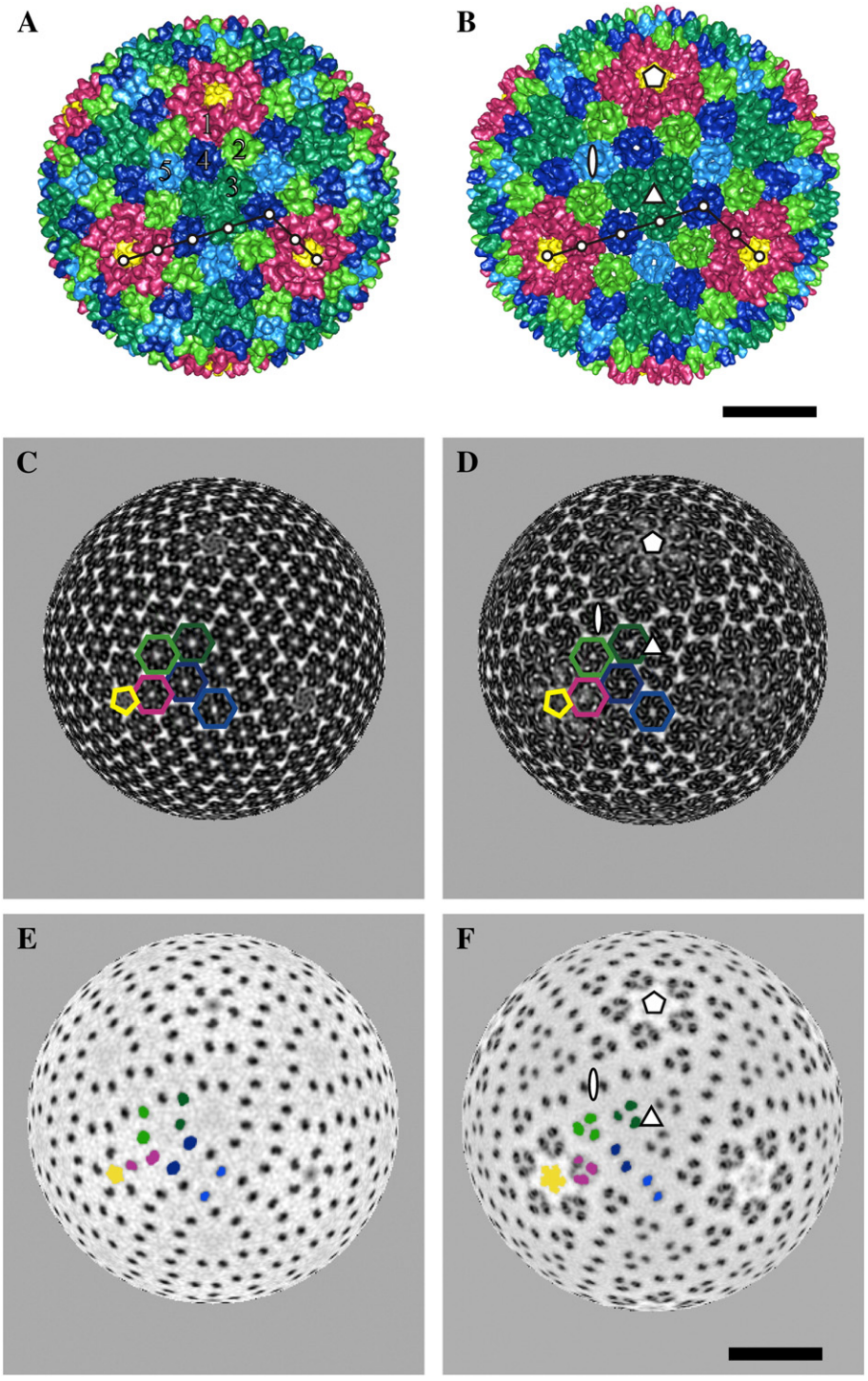

Fig. 5. Capsid architecture of P23-77 and SH1. (A) Surface representation of P23-77 drawn at 2 σ above mean of the intact particle reconstruction viewed down a 3-fold symmetry axis. (B) Surface representation of SH1 (Accession number EMD1353). Symmetry axes are indicated in B with a white ellipse (2-fold), triangle (3-fold) and pentagon (5-fold). The triangulation number (T) describes the geometrical arrangement of the capsomers, and is given by the relationship $T=h^2+hk+k^2$ (Caspar and Klug, 1962). The integers h and k that define the lattice points for a triangulation number $T=28$ *dextro* lattice ($h=4$, $k=2$) are depicted with white dots in A and B. Icosahedrally independent capsomers of P23-77 and SH1 have been manually segmented and are enumerated from 1 to 5. Wrigley (Wrigley, 1969) describes the arrangement of the icosahedral shell with the help of disymmetrons, trisymmetrons, and pentasymmetrons. Colored according to Wrigley's theory, the green capsomers (2 and 3) of P23-77 and SH1 correspond to trisymmetrons, the blue capsomers (4 and 5) to disymmetrons and the yellow and red (1) capsomers to pentasymmetrons. (C) A 0.28 nm thick spherical section of P23-77 at 37 nm and (D) of SH1 at 38 nm showing the hexameric bases of the capsomers. (E) A 0.28 nm thick spherical section of P23-77 at 40 nm and (F) of SH1 at 41 nm cutting through the decorating towers. (C-F) Bases and towers belonging to one asymmetric unit are coloured as in A and B. Bar, 20 nm.

corporation collection (Yu et al., 2006), and propagated in *Thermus thermophilus* (ATCC 33923). *T. thermophilus* cells were grown in thermus medium containing 4 g yeast extract, 8 g peptone, 2 g NaCl, (20 g agar when appropriate) per L at pH 7.5.

Virus propagation and purification

To obtain virus stocks, the soft-agar layer was harvested from semiconfluent plates incubated at 70 °C, 16 h in a humid

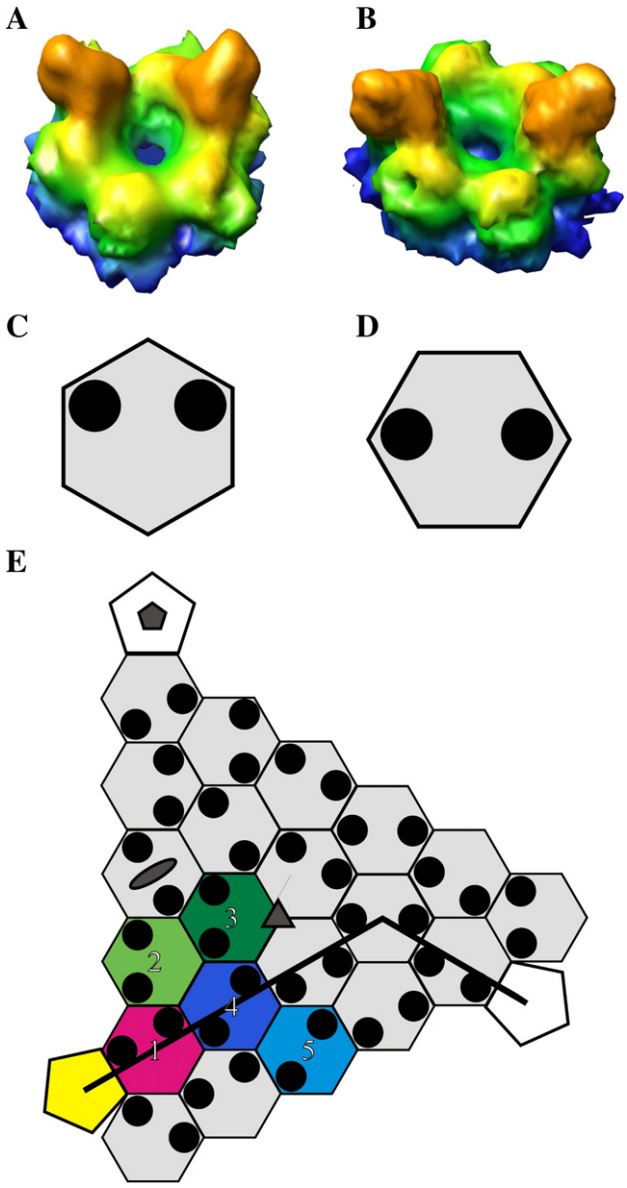

Fig. 6. Capsid architecture of P23-77. (A, B) The capsid of P23-77 is built up of two different hexameric capsomers, type A (A) and type B (B), that are decorated with two towers each (orange). (C) Schematic representation of the type A capsomers. (D) Schematic representation of the type B capsomers. (E) Schematic diagram of a P23-77 facet, with one asymmetric unit coloured. Each icosahedrally independent capsomer is assigned a colour and a number corresponding to those in Fig. 5A. Type A capsomers are colored in shades of green and red, and type B capsomers in shades of blue. The type B capsomer 5 is shared with the neighboring asymmetric unit. The black line indicates the lattice points for the $T=28$ *dextro* organisation of the P23-77 capsomers. Symmetry axes are indicated with an ellipse (2-fold), triangle (3-fold) and pentagon (5-fold). In C-E, the position of the capsomer towers is indicated with black dots on top of a hexagonal base.

environment (sealed plastic bags), by adding 3 ml of thermus medium per plate, followed by incubation for 4 h, with aeration, at 70 °C. The cell debris was removed by differential centrifugation (Sorvall GSA rotor, 7000 rpm, 20 min, 25 °C) and the supernatant was titered. For single cycle growth experiments, cells were infected at a multiplicity of infection (MOI) of about 10 at a cell density of 7×10^8 colony forming units (cfu)/ml. After lysis, cultures were cleared by centrifugation (Sorvall SLA3000 rotor, 7000 rpm, 20 min, 25 °C), and virus particles were precipitated from the supernatant by the addition of 12% w/v polyethylene glycol (PEG) 6000 and 0.5 M NaCl (final concentrations) with stirring for 35 min at 28 °C. The virus precipitate was collected by centrifugation (Sorvall SLA3000 rotor, 7000 rpm, 20 min, 25 °C) and the pellet subsequently rinsed with 20 mM Tris–HCl pH 7.5, 5 mM $MgCl_2$, 150 mM NaCl (TV buffer) and resuspended in 1/20 of the original lysate volume. All subsequent steps were carried out in the same buffer. Viruses were purified by rate zonal centrifugation (linear 5–20% (w/v) sucrose gradient, Sorvall AH629 rotor, 23000 rpm, 45 min, 25 °C). The light-scattering virus zone was collected (1× purified virus) or the gradient was fractionated to assay the protein content and infectivity. To produce 2× purified viruses, 10 ml of the 1× band was further purified by equilibrium centrifugation (linear 20–70% (w/v) sucrose gradient, Sorvall AH629 rotor, 23000 rpm, 17 h, 25 °C) or alternatively in 1.30 mg/ml CsCl in TV buffer (Sorvall AH629 rotor, 21000 rpm, 16 h, 25 °C). The light-scattering virus zone was collected, an equal volume of buffer was added, and virus particles were collected by differential centrifugation (Sorvall T647.5 rotor, 32000 rpm, 4 h, 25 °C). The obtained virus pellet was resuspended into TV buffer. Alternatively the gradients were fractionated and the fractions were assayed for protein content, density and infectivity.

Phage adsorption assay

The adsorption assay was carried out as previously described using fresh virus stocks (Adams, 1959). *T. thermophilus* cells were grown to a cell density of 7×10^8 cfu/ml and 200 µl of the cell suspension was mixed with ~200 infective phage particles, and the mixture was incubated at 70 or 22 °C. Samples were taken at different time points, cells removed by centrifugation (Eppendorf microcentrifuge, 5000 rpm, 4 min, 22 °C) and the number of nonadsorbed phage particles was determined in the supernatant by titering.

Protein analysis

The proteins in purified virus preparations were resolved using sodium dodecyl sulfate-polyacrylamide gel electrophoresis (SDS-PAGE; 16% acrylamide, (Olkkonen and Bamford, 1989); or tricine-SDS-PAGE (17% acrylamide; (Schägger and von Jagow, 1987) using a BIO-RAD Precision Plus Protein standard as a marker. Protein concentrations were determined with Coomassie brilliant blue using bovine serum albumin as a standard (Bradford, 1976).

Lipid analysis

Lipid analysis was carried out on all of the fractions (1 ml) from a sucrose equilibrium gradient. Lipids were extracted essentially as described previously (Folch et al., 1957), except that no NaCl was included in the washing steps. A hexane, diethyl ether and acetic acid mixture (80:20:1; v/v) was used as the solvent system for neutral lipids on silica gel plates (Silica gel 60; Merck) (Kates, 1972). The lipids on the thin layer silica plates were visualized by iodine vapour and scanned.

Electron microscopy

For thin-section electron microscopy *T. thermophilus* cells were grown to a density of 7×10^8 cfu/ml and infected with freshly made P23-77, P23-72 or P23-65H phage stocks at MOI 10 (45 and 70 min post-infection (p.i.) samples) or MOI 40 (15 min p.i. sample) at 70 °C. Samples were taken at different time points after infection and fixed with 3% (v/v) glutaraldehyde in 20 mM phosphate buffer (pH 7.4). After 20 min incubation at room temperature the fixed cells were collected, washed twice and prepared for transmission electron microscopy as previously described (Bamford and Mindich, 1980). Micrographs were taken with a JEOL 1200 EX electron microscope operating at 60 kV.

For cryo-EM, 1× and 2× purified P23-77 viruses were concentrated from gradient fractions by differential centrifugation (Beckman

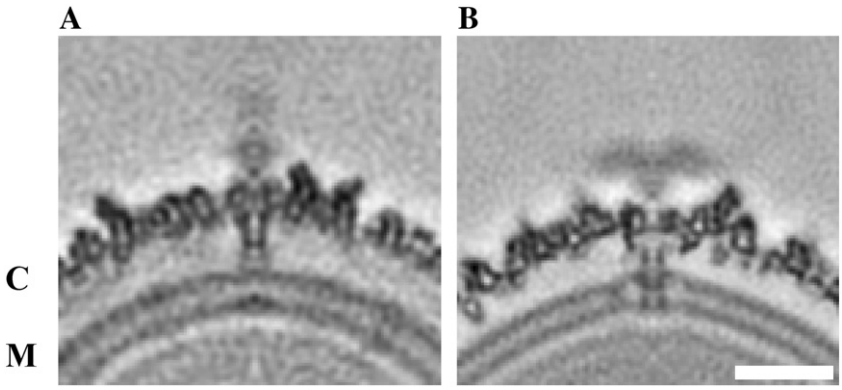

Fig. 7. Close-up of 0.84 nm thick central sections through the five-fold vertices of P23-77 (A) and SH1 (B). The position of the capsid (C) and membrane (M) are indicated. The P23-77 spike is stick-like compared to the bifurcated SH1 spike. Strong densities connecting the capsid to the membrane are visible in both SH1 and P23-77. Bar, 10 nm.

SW50.1 rotor, 40000 rpm, 40 min, 25 °C), resuspended in 20 mM Tris–HCl pH 7.5, 1 mM $MgCl_2$, 0.1 mM $CaCl_2$ (1× virus zone) or TV buffer (2× virus zone) and immediately used for the preparation of vitrified specimens. Aliquots of virus (3 μl) were vitrified on holey carbon film coated grids (Quantifoil R 2/2) in liquid ethane as described previously (Adrian et al., 1984). The specimens were imagined at −180 °C in a FEI Tecnai F20 field emission gun transmission electron microscope operating at 200 kV and using a Gatan 626 cryoholder. Virus images were recorded on Kodak SO163 film or on a Gatan UltraScan 4000 CCD camera under low dose conditions, at nominal magnifications of 50,000× and 68,000× respectively. The micrographs recorded on film were developed in full-strength Kodak D19 film developer for 12 min. All electron microscopy data were collected in the Electron Microscopy Unit, Institute of Biotechnology, University of Helsinki.

Image processing

Films were digitized at 7-μm intervals on a Zeiss Photoscan TD scanner, resulting in a nominal sampling of 0.14 nm $pixel^{-1}$ and binned to 0.28 nm $pixel^{-1}$. CCD sampling was 0.22 nm $pixel^{-1}$. CTFFIND3 (Mindell and Grigorieff, 2003) was used to estimate the contrast transfer function. Drifted and astigmatic pictures were discarded. ETHAN (Kivioja et al., 2000) was used to locate the virus particles, and particles were extracted in the EMAN program BOXER (Ludtke et al., 1999). Bsoft (Heymann, 2001) was used for further image processing unless stated otherwise.

The three-dimensional structure of the archaeal virus SH1 (Accession number EMD1353; (Jäälinoja et al., 2008), scaled to the appropriate size, was used as a starting model to determine the orientations and origins of the icosahedral particles in a model-based approach (Baker and Cheng, 1996). PFT2 and EM3DR2 (Baker and Cheng, 1996) were used in the initial rounds of refinement, and POR and P3DR (Ji et al., 2006; Marinescu and Ji, 2003) for subsequent rounds. The contrast transfer function was fully corrected in P3DR using a Wiener filter (Marinescu and Ji, 2003).

The spacing of the P23-77 protein and membrane layers was calculated from spherically-averaged radial profiles of the reconstructions using Bsoft (Heymann, 2001; Huiskonen et al., 2004). Bsoft (Heymann, 2001) was in addition used to create spherical and central sections of the three-dimensional models of P23-77 and SH1 (Accession number EMD1353).

Segmentation of the reconstruction and mass estimates of the capsomers was carried out as described previously (Jäälinoja et al., 2008). The molecular mass for the P23-77 capsomers was estimated in EMAN using a density threshold of 2 standard deviations above the mean and a protein density of 1.35 g/ml (Ludtke et al., 1999). All surface representations were created with the UCSF Chimera package (Pettersen et al., 2004).

The reconstruction of the virion has been deposited in the EMDB, at the European Bioinformatics Institute with the accession code: EMD1525.

Acknowledgments

The technical assistance of Anna Latva-Käyrä and Heini Hyvönen is gratefully acknowledged. Harri Jäälinoja and Jani Seitsonen are acknowledged for the useful discussions. We thank the Electron Microscopy Unit of the Institute of Biotechnology, University of Helsinki for providing microscopy facilities. This study was supported (to S.J.B and D.H.B) from the Finnish Center of Excellence Program [2006–2011] grant 1213467. Further funding was obtained from the Academy of Finland [grant 1210253] to D.H.B and grant 1112244 to S. J. B. As part of the European Science Foundation EUROCORES Programme Euro-SCOPE, the work is also supported by funds from the European Commission's Sixth Framework Programme under contract ERAS-CT-2003-980409. The Helsinki Graduate School of Biotechnology and Molecular Biology is acknowledged for funding of S.T.J.

References

Abrescia, N.G., Cockburn, J.J., Grimes, J.M., Sutton, G.C., Diprose, J.M., Butcher, S.J., Fuller, S.D., San Martin, C., Burnett, R.M., Stuart, D.I., Bamford, D.H., Bamford, J.K., 2004. Insights into assembly from structural analysis of bacteriophage PRD1. Nature 432, 68–74.

Ackermann, H.W., 2007. 5500 Phages examined in the electron microscope. Arch. Virol. 152, 227–243.

Adams, M.H., 1959. Bacteriophages. Interscience publishers, Inc., New York.

Adrian, M., Dubochet, J., Lepault, J., McDowall, A.W., 1984. Cryo-electron microscopy of viruses. Nature 308, 32–36.

Baker, T.S., Cheng, R.H., 1996. A model-based approach for determining orientations of biological macromolecules imaged by cryoelectron microscopy. J. Struct. Biol. 116, 120–130.

Bamford, D.H., 2005. Tectiviridae. In: Fauquet, C.M., Mayo, M.A., Maniloff, J., Desselberger, U., Ball, L.A. (Eds.), Virus taxonomy, Eighth report of the international committee on taxonomy of viruses. Elsevier Academic Press, London, pp. 81–85.

Bamford, J.K., Bamford, D.H., 1991. Large-scale purification of membrane-containing bacteriophage PRD1 and its subviral particles. Virology 181, 348–352.

Bamford, D.H., Mindich, L., 1980. Electron microscopy of cells infected with nonsense mutants of bacteriophage phi 6. Virology 107, 222–228.

Bamford, D.H., Burnett, R.M., Stuart, D.I., 2002. Evolution of viral structure. Theor. Popul. Biol 61, 461–470.

Bamford, D.H., Grimes, J.M., Stuart, D.I., 2005a. What does structure tell us about virus evolution? Curr. Opin. Struct. Biol. 15, 655–663.

Bamford, D.H., Ravantti, J.J., Ronnholm, G., Laurinavicius, S., Kukkaro, P., Dyall-Smith, M., Somerharju, P., Kalkkinen, N., Bamford, J.K., 2005b. Constituents of SH1, a novel lipid-containing virus infecting the halophilic euryarchaeon *Haloarcula hispanica*. J. Virol. 79, 9097–9107.

Benson, S.D., Bamford, J.K., Bamford, D.H., Burnett, R.M., 1999. Viral evolution revealed by bacteriophage PRD1 and human adenovirus coat protein structures. Cell 98, 825–833.

Benson, S.D., Bamford, J.K., Bamford, D.H., Burnett, R.M., 2004. Does common architecture reveal a viral lineage spanning all three domains of life? Mol. Cell 16, 673–685.

Blondal, T., Thorisdottir, A., Unnsteinsdottir, U., Hjorleifsdottir, S., Aevarsson, A., Ernstsson, S., Fridjonsson, O.H., Skirnisdottir, S., Wheat, J.O., Hermannsdottir, A.G., Sigurdsson, S.T., Hreggvidsson, G.O., Smith, A.V., Kristjansson, J.K., 2005. Isolation and characterization of a thermostable RNA ligase 1 from a *Thermus scotoductus* bacteriophage TS2126 with good single-stranded DNA ligation properties. Nucleic Acids Res. 33, 135–142.

Bradford, M.M., 1976. A rapid and sensitive method for the quantitation of microgram quantities of protein utilizing the principle of protein-dye binding. Anal. Biochem. 72, 248–254.

Briggs, J.A., Huiskonen, J.T., Fernando, K.V., Gilbert, R.J., Scotti, P., Butcher, S.J., Fuller, S.D., 2005. Classification and three-dimensional reconstruction of unevenly distributed or symmetry mismatched features of icosahedral particles. J. Struct. Biol. 150, 332–339.

Brock, T.D., 2005. Genus Thermus. In: Holt, J.G. (Ed.), Bergey's manual of systematic bacteriology, vol. 1. Williams & Wilkins, pp. 333–337.

Caspar, D.L., Klug, A., 1962. Physical principles in the construction of regular viruses. Cold Spring Harb. Symp. Quant. Biol. 27, 1–24.

Cerritelli, M.E., Cheng, N., Rosenberg, A.H., McPherson, C.E., Booy, F.P., Steven, A.C., 1997. Encapsidated conformation of bacteriophage T7 DNA. Cell 91, 271–280.

Chang, J., Weigele, P., King, J., Chiu, W., Jiang, W., 2006. Cryo-EM asymmetric reconstruction of bacteriophage P22 reveals organization of its DNA packaging and infecting machinery. Structure 14, 1073–1082.

Cockburn, J.J., Abrescia, N.G., Grimes, J.M., Sutton, G.C., Diprose, J.M., Benevides, J.M., Thomas Jr., G.J., Bamford, J.K., Bamford, D.H., Stuart, D.I., 2004. Membrane structure and interactions with protein and DNA in bacteriophage PRD1. Nature 432, 122–125.

Folch, J., Lees, M., Sloane Stanley, G.H., 1957. A simple method for the isolation and purification of total lipides from animal tissues. J. Biol. Chem. 226, 497–509.

Grahn, M.A., Butcher, S.J., Bamford, J.H.K., Bamford, D.H., 2006. PRD1: Dissecting the genome, structure and entry. In: Calendar, R. (Ed.), The Bacteriophages. Oxford University Press, pp. 161–170.

Heymann, J.B., 2001. Bsoft: image and molecular processing in electron microscopy. J. Struct. Biol. 133, 156–169.

Hreggvidsson, G.O., Skirnisdottir, S., Smit, B., Hjorleifsdottir, S., Marteinsson, V.T., Petursdottir, S., Kristjansson, J.K., 2006. Polyphasic analysis of Thermus isolates from geothermal areas in Iceland. Extremophiles 10, 563–575.

Huiskonen, J.T., Butcher, S.J., 2007. Membrane-containing viruses with icosahedrally symmetric capsids. Curr. Opin. Struct. Biol. 17, 229–236.

Huiskonen, J.T., Kivela, H.M., Bamford, D.H., Butcher, S.J., 2004. The PM2 virion has a novel organization with an internal membrane and pentameric receptor binding spikes. Nat. Struct. Mol. Biol. 11, 850–856.

Huiskonen, J.T., Jaalinoja, H.T., Briggs, J.A., Fuller, S.D., Butcher, S.J., 2007a. Structure of a hexameric RNA packaging motor in a viral polymerase complex. J. Struct. Biol. 158, 156–164.

Huiskonen, J.T., Manole, V., Butcher, S.J., 2007b. Tale of two spikes in bacteriophage PRD1. Proc. Natl. Acad. Sci. U S A 104, 6666–6671.

Jäälinoja, H.T., Roine, E., Laurinmäki, P., Kivelä, H.M., Bamford, D.H., Butcher, S.J., 2008. Structure and host cell interaction of SH1, a membrane-containing, halophilic euryarchaeal virus. Proc. Natl. Acad. Sci. USA 105, 8008–8013.

Ji, Y., Marinescu, D.C., Zhang, W., Zhang, X., Yan, X., Baker, T.S., 2006. A model-based parallel origin and orientation refinement algorithm for cryoTEM and its application to the study of virus structures. J. Struct. Biol. 154, 1–19.

Kates, M., 1972. Techniques of lipidology: Isolation, analysis and identification of lipids. North-Holland Publishing Company, Amsterdam.

Khayat, R., Tang, L., Larson, E.T., Lawrence, C.M., Young, M., Johnson, J.E., 2005. Structure of an archaeal virus capsid protein reveals a common ancestry to eukaryotic and bacterial viruses. Proc. Natl. Acad. Sci. U S A 102, 18944–18949.

Kivela, H.M., Mannisto, R.H., Kalkkinen, N., Bamford, D.H., 1999. Purification and protein composition of PM2, the first lipid-containing bacterial virus to be isolated. Virology 262, 364–374.

Kivioja, T., Ravantti, J., Verkhovsky, A., Ukkonen, E., Bamford, D., 2000. Local average intensity-based method for identifying spherical particles in electron micrographs. J. Struct. Biol. 131, 126–134.

Laurinmaki, P.A., Huiskonen, J.T., Bamford, D.H., Butcher, S.J., 2005. Membrane proteins modulate the bilayer curvature in the bacterial virus Bam35. Structure 13, 1819–1828.

Ludtke, S.J., Baldwin, P.R., Chiu, W., 1999. EMAN: semiautomated software for high-resolution single-particle reconstructions. J. Struct. Biol. 128, 82–97.

Maaty, W.S., Ortmann, A.C., Dlakic, M., Schulstad, K., Hilmer, J.K., Liepold, L., Weidenheft, B., Khayat, R., Douglas, T., Young, M.J., Bothner, B., 2006. Characterization of the archaeal thermophile Sulfolobus turreted icosahedral virus validates an evolutionary link among double-stranded DNA viruses from all domains of life. J. Virol. 80, 7625–7635.

Marinescu, D.C., Ji, Y., 2003. A computational framework for the 3D structure determination of viruses with unknown symmetry. J. Parallel. Distrib. Comput. 63, 738–758.

Mindell, J.A., Grigorieff, N., 2003. Accurate determination of local defocus and specimen tilt in electron microscopy. J. Struct. Biol. 142, 334–347.

Nandhagopal, N., Simpson, A.A., Gurnon, J.R., Yan, X., Baker, T.S., Graves, M.V., Van Etten, J.L., Rossmann, M.G., 2002. The structure and evolution of the major capsid protein of a large, lipid-containing DNA virus. Proc. Natl. Acad. Sci. U S A 99, 14758–14763.

Olkkonen, V.M., Bamford, D.H., 1989. Quantitation of the adsorption and penetration stages of bacteriophage phi 6 infection. Virology 171, 229–238.

Pantazaki, A.A., Pritsa, A.A., Kyriakidis, D.A., 2002. Biotechnologically relevant enzymes from Thermus thermophilus. Appl. Microbiol. Biotechnol. 58, 1–12.

Pask-Hughes, R., Williams, R.A., 1975. Extremely thermophilic gram-negative bacteria from hot tap water. J. Gen. Microbiol. 88, 321–328.

Pederson, D.M., Welsh, L.C., Marvin, D.A., Sampson, M., Perham, R.N., Yu, M., Slater, M.R., 2001. The protein capsid of filamentous bacteriophage PH75 from Thermus thermophilus. J. Mol. Biol. 309, 401–421.

Pettersen, E.F., Goddard, T.D., Huang, C.C., Couch, G.S., Greenblatt, D.M., Meng, E.C., Ferrin, T.E., 2004. UCSF Chimera–a visualization system for exploratory research and analysis. J. Comput. Chem. 25, 1605–1612.

Rachel, R., Bettstetter, M., Hedlund, B.P., Haring, M., Kessler, A., Stetter, K.O., Prangishvili, D., 2002. Remarkable morphological diversity of viruses and virus-like particles in hot terrestrial environments. Arch. Virol. 147, 2419–2429.

Ramaley, R.F., Hixson, J., 1970. Isolation of a nonpigmented, thermophilic bacterium similar to Thermophilic bacterium similar to Thermus aquaticus. J. Bacteriol. 103, 527–528.

Ravantti, J.J., Gaidelyte, A., Bamford, D.H., Bamford, J.K., 2003. Comparative analysis of bacterial viruses Bam35, infecting a gram-positive host, and PRD1, infecting gram-negative hosts, demonstrates a viral lineage. Virology 313, 401–414.

Ray, P.H., White, D.C., Brock, T.D., 1971. Effect of growth temperature on the lipid composition of Thermus aquaticus. J. Bacteriol. 108, 227–235.

Rice, G., Tang, L., Stedman, K., Roberto, F., Spuhler, J., Gillitzer, E., Johnson, J.E., Douglas, T., Young, M., 2004. The structure of a thermophilic archaeal virus shows a double-stranded DNA viral capsid type that spans all domains of life. Proc. Natl. Acad. Sci. U S A 101, 7716–7720.

Romancer, M., Gaillard, M., Geslin, C., Prieur, D., 2007. Viruses in extreme environmets. Rev. Environ. Sci. Biotechnol. 6, 17–31.

Sakaki, Y., Oshima, T., 1975. Isolation and characterization of a bacteriophage infectious to an extreme thermophile, Thermus thermophilus HB8. J. Virol. 15, 1449–1453.

Schägger, H., von Jagow, G., 1987. Tricine-sodium dodecyl sulfate-polyacrylamide gel electrophoresis for the separation of proteins in the range from 1 to 100 kDa. Anal. Biochem. 166, 368–379.

Simpson, A.A., Nandhagopal, N., Van Etten, J.L., Rossmann, M.G., 2003. Structural analyses of Phycodnaviridae and Iridoviridae. Acta Crystallogr. D Biol. Crystallogr. 59, 2053–2059.

Wrigley, N.G., 1969. An electron microscope study of the structure of Sericesthis iridescent virus. J. Gen. Virol. 5, 123–134.

Yan, X., Olson, N.H., Van Etten, J.L., Bergoin, M., Rossmann, M.G., Baker, T.S., 2000. Structure and assembly of large lipid-containing dsDNA viruses. Nat. Struct. Biol. 7, 101–103.

Yu, M.X., Slater, M.R., Ackermann, H.W., 2006. Isolation and characterization of Thermus bacteriophages. Arch. Virol. 151, 663–679.